Hydromagnetic flow of a Cu–water nanofluid past a moving wedge with viscous dissipation

A. M. Salem[a)b)†], Galal Ismail[c)], and Rania Fathy[c)]

[a)] Department of Mathematics, Faculty of Science and Arts, Qassim University, Al-Muznib, Saudi Arabia
[b)] Department of Basic Science, Faculty of Computers and Informatics, Suez Canal University, Egypt
[c)] Department of Mathematics, Faculty of Science, Zagazig University, Egypt

(Received 3 June 2013; revised manuscript received 18 July 2013; published online 20 February 2014)

A numerical study is performed to investigate the flow and heat transfer at the surface of a permeable wedge immersed in a copper (Cu)–water-based nanofluid in the presence of magnetic field and viscous dissipation using a nanofluid model proposed by Tiwari and Das (Tiwari I K and Das M K 2007 *Int. J. Heat Mass Transfer* **50** 2002). A similarity solution for the transformed governing equation is obtained, and those equations are solved by employing a numerical shooting technique with a fourth-order Runge–Kutta integration scheme. A comparison with previously published work is carried out and shows that they are in good agreement with each other. The effects of velocity ratio parameter λ, solid volume fraction φ, magnetic field M, viscous dissipation E_c, and suction parameter F_w on the fluid flow and heat transfer characteristics are discussed. The unique and dual solutions for self-similar equations of the flow and heat transfer are analyzed numerically. Moreover, the range of the velocity ratio parameter for which the solution exists increases in the presence of magnetic field and suction parameter.

Keywords: nanofluid, dual solution, magnetic field, viscous dissipation

PACS: 44.20.+b, 44.30.+v, 47.65.−d, 47.61.−k **DOI:** 10.1088/1674-1056/23/4/044402

1. Introduction

Common heat transport fluids such as water, ethylene glycol, end engine oil have limited heat transfer capabilities due to their low heat transfer properties. In contrast, metals have thermal conductivities up to three times higher than these fluids, so it is natural that it would be desired to combine the two substances to produce a heat transfer medium that behaves like a fluid, but has the thermal conductivity of a metal. A mixture of nano-size particle suspended in a base fluid is named nanofluid and was firstly reported by Choi.[1] Nanofluid, where heat transfer can be reduced or enhanced at will, can be utilized where straight heat transfer enhancement is very important in many industrial applications, nuclear reactors, transportation as well as electronics and biomedicine. Nanofluids can be also used for cooling microchips in computers, and in other areas. They can be used in various biomedical applications like cancer therapeutics, nano-drug delivery, nanocryosurgery, and cryopreservation. The broad ranges of current and future applications involving nanofluids have been given by Wong and Leone.[2] Many researchers have studied and reported results on convective heat transfer in nanofluids considering various flow conditions in different geometries.[3–9] A comprehensive study of convective transport in nanofluids was made by Buongiorno.[10] Kuznetsov and Nield[11] presented a similarity solution of natural convective boundary-layer flow of a nanofluid past a vertical plate. Abu-Nada and Oztop[12] investigated numerically the effect of a Cu-water nanofluid on natural convection heat transfer in an inclined cavity. They used the inclination angle as a control parameter for flow and heat transfer in the cavity.

The boundary layer flow over a static or moving wegde in a viscous fluid has been considered by Riely and Weidman[13] and Yacob and Ishak,[14] which is an extension of the flow over a static wedge considered by Falkner and Skan.[15] They developed a similarity transformation that can be used to reduce the partial differential boundary layer equations and then solved them numerically. Magnetic fields are widely used in modern metallurgical and metal-working processes such as magnetohydrodynamic (MHD) pumps, MHD power generators, flow meters, the cooling of reactors, etc. Many mathematic models have been proposed to explain the behaviors of the viscous MHD flow over a wedge under different conditions.[16–19] Recently, Xiaohong *et al.*[20] studied the MHD mixed convection heat transfer over a permeable stretching wedge with thermal radiation. Hamad *et al.*[21] analyzed the magnetic field effects on the free convection flow of nanofluid past a vertical semi-infinite flat plate.

In addition to magnetic field, one has to consider the effect of viscous dissipation on the boundary layer flow since this has a direct influence on the heat transfer rate. Gebhart[22] was first to study the problem by taking into account the viscous dissipation and also defined the non-dimensional dissipation parameter. Pantokratoras[23] studied the effect of vis-

†Corresponding author. E-mail: azizsalem32@hotmail.com

© 2014 Chinese Physical Society and IOP Publishing Ltd

cous dissipation in natural convection along a heated vertical plate. Zueco and Beg[24] considered the network simulation solutions for laminar radiating dissipative magneto-gas dynamic heat transfer over a wedge in a non-Darcian porous region. Muhaimin *et al.*[25] investigated the influences of thermal stratification and variable viscosity on a non-Darcy convective heat transfer past a porous wedge in the presence of viscous dissipation. Chandrasekar and Baskaran[26] studied the effect of viscous dissipation and stress work on the MHD boundary layer flow over a wedge. Makinde[27] studied the effect of viscous dissipation on boundary layer flow over a moving flat plate for two types of water-based Newtonian nanofluids containing metallic or nonmetallic nanoparticles such as copper (Cu) and titania (TiO_2). They observed that the viscous dissipation effect reduces the wall heat transfer rate and enhances the wall mass transfer rate.

In the present paper we numerically investigate the flow and heat transfer at the surface of a Pbermeable wedge immersed in a Cu–water nanofluid in the presence of viscous dissipation and magnetic field using a nanofluid model proposed by Tiwari and Das,[6] which was also used by several authors such as Oztop and Abu-Nada,[8] Muthtamilselvan *et al.*,[9] and Abu-Nada and Oztop.[12] The similarity transformation is utilized to convert the governing partial differential equations into ordinary differential equations and then the resulting equations are solved numerically. This problem represents a generalization of the problem considered by Yacob *et al.*[14] through the inclusion of magnetic field, viscous dissipation, and mass transfer at the wedge.

2. Formulation of the problem

Consider a steady two-dimensional laminar boundary layer flow of an incompressible viscous nanofluid (Cu–water) moving over the surface of a permeable wedge in the presence of viscous dissipation and magnetic field $B(x)$. The magnetic field acts transversely on the flow. The magnetic Renolds number is considered to be small so that the induced magnetic field is negligible. It is also assumed that the external electric field is zero and the electric field due to polarization of charges is negligible. Further, it is assumed that the velocity of the ambient fluid is $u_e(x) = U_\infty x^m$ and the velocity of the moving wedge is $u_w(x) = U_w x^m$, where U_∞, U_w, and m are all constant with $0 \leq m \leq 1$. The positive x coordinate is measured along the surface of the wedge with the apex as the origin, and the positive y coordinate is measured normal to the x axis in the outward direction towards the fluid. It is assumed that the base fluid and the nanoparticles are in thermal equilibrium and no slip occurs between them. The thermophysical properties of the fluid and nanoparticles are given in Table 1.[8] Under these assumptions and using the model of the nanofluid proposed by Tiwari and Das,[6] the velocity and temperature fields in the boundary layer are governed by the two-dimensional boundary layer equations for mass, momentum, and thermal energy as follows:

$$\frac{\partial u}{\partial x} + \frac{\partial v}{\partial y} = 0, \tag{1}$$

$$u\frac{\partial u}{\partial x} + v\frac{\partial u}{\partial y} = u_e(x)\frac{\partial u_e(x)}{\partial x} + \frac{\mu_{nf}}{\rho_{nf}}\frac{\partial^2 u}{\partial y^2} - \frac{\sigma B^2(x)}{\rho_{nf}}(u - U(x)), \tag{2}$$

$$u\frac{\partial T}{\partial x} + v\frac{\partial T}{\partial y} = \alpha_{nf}\frac{\partial^2 T}{\partial y^2} + \frac{\mu_{nf}}{(\rho c_p)_{nf}}\left(\frac{\partial u}{\partial y}\right)^2, \tag{3}$$

where u and v are velocity components along the x and y axes, respectively, T is the temperature of the nanofluid in the boundary layer, T_∞ is the temperature of the ambient fluid outside the boundary layer, σ is the magnetic permeability and the magnetic field is given by $B(x) = B_0 x^{(m-1)/2}$, with B_0 being constant, ρ_{nf} and μ_{nf} are the density and effective viscosity of the nanofluid, α_{nf} and ν_{nf} are the thermal diffusivity and kinematic viscosity, respectively, which are defined as follows (see Khanafer *et al.*[3]):

$$\begin{aligned}
&\nu_{nf} = \frac{\mu_{nf}}{\rho_{nf}}, \quad \rho_{nf} = (1-\varphi)\rho_f + \varphi\rho_s,\\
&\mu_{nf} = \frac{\mu_f}{(1-\varphi)^{2.5}}, \quad \alpha_{nf} = \frac{k_{nf}}{(\rho c_p)_{nf}},\\
&\rho c_p = (1-\varphi)(\rho c_p)_f + \varphi(\rho c_p)_s\frac{k_{nf}}{k_f}\\
&\quad = \frac{(k_s+2k_f) - 2\varphi(k_f - k_s)}{(k_s+2k_f) + 2\varphi(k_f - k_s)},
\end{aligned} \tag{4}$$

where φ is the solid volume friction of the nanofluid, μ_f is the viscosity of the basic fluid, ρ_f and ρ_s are the densities of the pure fluid and nanoparticle, respectively, $(\rho c_p)_f$ and $(\rho c_p)_s$ are the specific heat parameters of the basic fluid and nanoparticle, respectively, and k_f and k_s are the thermal conductivities of the basic fluid and nanoparticle, respectively.

Table 1. Thermophysical properties of the base fluid and the nanoparticles.

Physical properties	Fluid phase (water)	Cu
c_p/(J/kg·K)	4179	385
ρ/(kg/m^3)	997.1	8933
k/(W/mK)	0.613	400
$\alpha/10^7$ (m^2/s)	1.47	1163.1

The appropriate boundary conditions for the problem are given by

$$\begin{aligned}
&u = u_w(x) = U_w x^m, \quad v = V_w, \quad T = T_w, \quad \text{at} \quad y = 0,\\
&u = u_e(x) = U_\infty x^m, \quad T \to T_\infty \quad \text{as} \quad y \to \infty,
\end{aligned} \tag{5}$$

where $m = \beta(2-\beta)$, β is the Hartree pressure gradient parameter that corresponds to $\beta = \Omega/\pi$ for a total angle Ω of

the wedge, V_w is the suction or blowing velocity across the surface of the boundary wall as $V_w < 0$ for suction and $V_w > 0$ for blowing.

The continuity equation (1) is satisfied by introducing a stream function $\psi(x,y)$ such as

$$u = \frac{\partial \psi}{\partial y}, \quad v = -\frac{\partial \psi}{\partial x}. \tag{6}$$

The following similarity variables are also introduced:

$$\psi = \left[\frac{2\nu_f x u_e(x)}{m+1}\right]^{1/2} f(\eta),$$
$$\eta = \left[\frac{(m+1)u_e(x)}{2\nu_f x}\right]^{1/2} y, \quad \theta = \frac{T-T_\infty}{T_w - T_\infty}, \tag{7}$$

where ν_f is the kinematic viscosity of the fluid. Substituting Eq. (7) into Eqs. (2) and (3), we obtain the following ordinary differential equations:

$$f''' = (1-\varphi)^{2.5}\left(1-\varphi+\varphi\frac{\rho_s}{\rho_f}\right) \times \left(\frac{2m}{m+1}(f'^2-1) - ff'' + M(f'-1)\right), \tag{8}$$

$$f\theta' + \frac{1}{p_r\left(1-\varphi+\varphi\frac{(\rho\rho_p)_s}{(\rho\rho_p)_f}\right)}\left(\frac{k_{nf}}{k_f}+\frac{4}{3R}\right)\theta'' + E_c f''^2 = 0, \tag{9}$$

subject to the following boundary conditions:

$$f(\eta) = F_w, \quad f'(\eta) = \lambda, \quad \theta(\eta) = 1 \quad \text{at} \quad \eta = 0,$$
$$F'(\eta) = 1, \quad \theta(\eta) = 0 \quad \text{as} \quad \eta \to \infty, \tag{10}$$

where $Pr = \nu_f/\alpha_f$ is the Prandtl number,

$$M = \frac{2\sigma B_o^2}{\rho_{nf} U_\infty (m+1)}$$

is the magnetic field, $E_c = u_e^2/[(c_p)_{nf}(T_w - T_\infty)]$ is the Eckert number, $F_w = -V_w/\sqrt{2x/(m+1)\nu_f u_w}$ is the dimensionless wall mass transfer coefficient, $\lambda = U_w/U_\infty$ is the ratio of the wall velocity to the free stream fluid velocity, $\lambda(>0)$ corresponds to the case where the wedge moves in the same direction as that the free stream moves in, and $\lambda(<0)$ when the wedge moves in the opposite direction to that the free stream moves in, while $\lambda = 0$ corresponds to a static wedge.

Important physical parameters for this flow and heat transfer case are the local skin-friction coefficient and the local Nusselt number which are defined as

$$c_f = \frac{\tau_w}{\rho_f (u_e(x))^2}, \quad Nu_x = \frac{x q_w}{k_f(T_w - T_\infty)}, \tag{11}$$

where

$$\tau_w = \mu_{nf}\left[\frac{\partial u}{\partial y}\right]_{y=0}, \quad q_w = -k_{nf}\left[\frac{\partial T}{\partial y}\right]_{y=0}$$

are shear stress and surface heat flux respectively. Using the new similarity variables in Eq. (8) gives

$$c_f[2Re_x/(m+1)]^{1/2} = \frac{1}{(1-\varphi)^{2.5}} f''(0),$$
$$Nu_x[(m+1)Re_x/2]^{-1/2} = -\frac{k_{nf}}{k_f}\theta'(0), \tag{12}$$

where $Re_x = u_e x/\nu_f$ is the local Reynolds number.

3. Results and discussion

The governing boundary layer equations (8) and (9) with boundary conditions (Eq. (10)) are solved numerically. Highly nonlinear momentum boundary layer equation and thermal boundary layer equation are converted into similarity equations and then solved numerically by using the modified fourth order Rung–Kutta method with the shooting technique.[28] In the shooting technique, the dual solutions are obtained by setting different initial guesses for the values of $f''(0)$ and $\theta'(0)$, where all profiles satisfy the far field boundary conditions (Eq. (10)) asymptotically but with different shapes. If $\varphi = 0$ (regular fluid), equation (8) reduces to the problem studied by Falkner and Skan.[15] Further, when $F_w = 0$ (without suction), $E_c = 0$ (without viscous dissipation) and $M = 0$ (without magnetic field), equations (8) and (9) reduce to those found by Yaco *et al.*[14] To assess the accuracy of the present results, a comparison of the wall shear stress results with the previously published data[29,30] for the case of $\varphi = M = E_c = 0$ and $F_w = 0$ is made. The comparison is shown in Table 2 and a good agreement is observed. Because of the lack of experimental data, the values of the parameters are chosen according to those given by previous investigators.

Table 2. Comparison of the values of $f''(0)$ for various values of λ with previous ones when $\varphi = M = E_c = 0$ and $F_w = 0$.

λ	Wang[29]		Bachok *et al.*[30]		Present results	
	First solution	Second solution	First solution	Second solution	First solution	Second solution
−1	1.32882	0	1.3288170	0	−1.3288165	0
−1.1	–	–	1.1866805	0.0492290	1.18667942	0.04921902
−1.15	1.08223	0.116702	1.0822315	0.1167022	1.08223091	0.11670207
−1.2	–	–	0.9324739	0.2336497	0.93247322	0.23364982
−1.2465	0.55430	0.116702	0.5842956	0.5542825	0.58430171	0.55429563
−1.24657	–	–	0.5639733	–	0.57458634	0.56402461

The computations are carried out for a Cu–water nanofluid for different values of velocity ratio parameter λ, solid friction of the nanofluid φ, magnetic parameter M, Eckert number E_c, and the dimensionless wall mass transfer F_w. The numerical computation results are given in Figs. 1–13 to have a great insight into the qualitative analysis of the results for $Pr = 6.2$ which represents water (basic fluid) at room temperature.

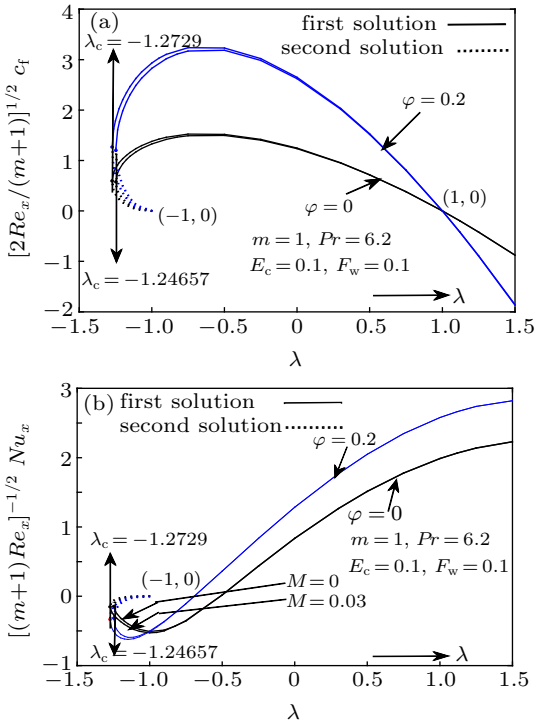


Fig. 1. (color online) Plots of shear stress (a) and temperature gradient (b) versus λ for various values of M and φ.

The plots of the skin friction coefficient and the local Nusselt number versus the velocity ratio parameter λ with $m = 1$ and $Pr = 6.2$ for different values of φ, E_c, and F_w in the absence and presence of magnetic effect are shown in Figs. 1–3. These figures show that there are regions of unique solutions for $\lambda > -1$, dual solutions for $\lambda_c < \lambda \leq -1$, and for $\lambda < \lambda_c$, the boundary layer theory breaks down and equations (8) and (9) become unsolvable, where λ_c represents the minimum values of λ for which the solution exists. Also, we observe that for positive values of λ (the wedge and the fluid move in the same direction), the magnetic field does not affect the wall shear stress $f''(0)$ nor the wall heat transfer $-\theta'(0)$, while for negative values of λ ($\lambda \geq \lambda_c$) the magnetic field has significant effects on $f''(0)$ and $-\theta'(0)$. It can also be seen that, all the solutions pass through $f''(0) = 0$ when $\lambda = 1$ (Figs. 1(a) and 3(a)). Physically, this point corresponds to zero friction in the boundary layer because the wedge and the fluid move with the same velocity. This observation is in agreement with that obtained by yacob *et al.*[14] and Bachok *et al.*[30] Also, figures 1–3 show that the values of λ_c do not depend on the nanoparticle volume friction nor viscous dissipation parameters but they depend on the parameters M and F_w. Based on our computation, $\lambda_c = -1.24657$ when $F_w = 0$ (without suction), $M = 0$ (without magnetic field), $E_c = 0, 0.1, 0.5$ and $\varphi = 0, 0.2$. This value of λ_c is in agreement with the result reported by Bachok *et al.*[30] For $M = 0.03$, $\lambda_c = -1.2729$ when $F_w = 0$. Also, for hydrodynamic flow ($M = 0$), the values of λ_c, when $F_w = 0.1$ and $F_w = 0.2$, are $\lambda_c = -1.3$ and $\lambda_c = -1.3643$ respectively. For magnetohydrodynamic flow ($M \neq 0$), $\lambda_c = -1.3291$ and -1.39 for $F_w = 0.1$ and $F_w = 0.2$, respectively. These results show that $|\lambda_c|$ increases with the increasing of M and F_w. Thus the effects of magnetic field and suction parameters are to increase the range of λ ($\lambda < -1$) for which dual solution exists.

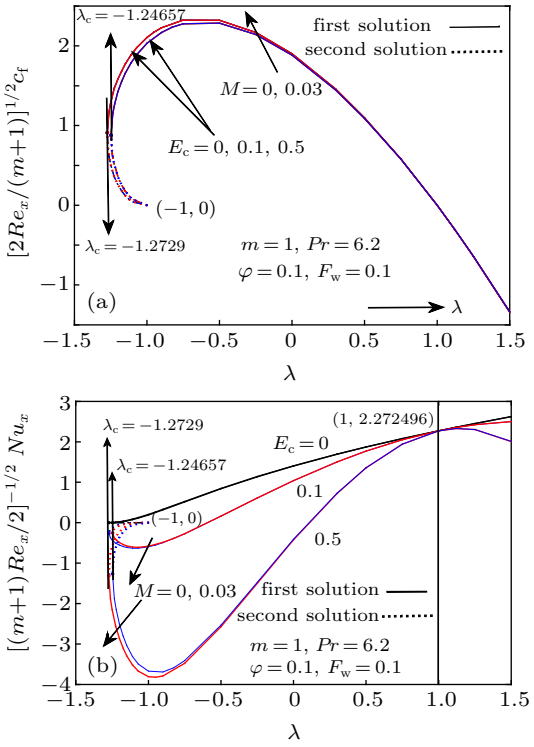


Fig. 2. (color online) Plots of shear stress (a) and temperature gradient (b) versus λ for various values of M and E_c.

Since viscous dissipation does not occur explicitly in the momentum equation, its effect on the wall shear stress is negligible as shown in Fig. 2(a). In the absence of viscous dissipation, figure 2(b) shows that the variation of the magnetic field induces the weak influence on the temperature gradient of the fluid at the surface of the wedge. However, when the internal heating of viscous dissipation is taken into account, the temperature gradient at the surface is a strong function of magnetic field as shown in Fig. 2(b), which means that the heat transfer rate at the surface is dependent on the magnetic field when the wedge and free stream move in the opposite

directions. Also, we notice from this figure that all curves in Fig. 2(b) intersect at point (1, 2.27249618), which means that the temperature gradient is equal and independent of the viscous dissipation when the wedge and the fluid move with the same velocity ($\lambda = 1$).

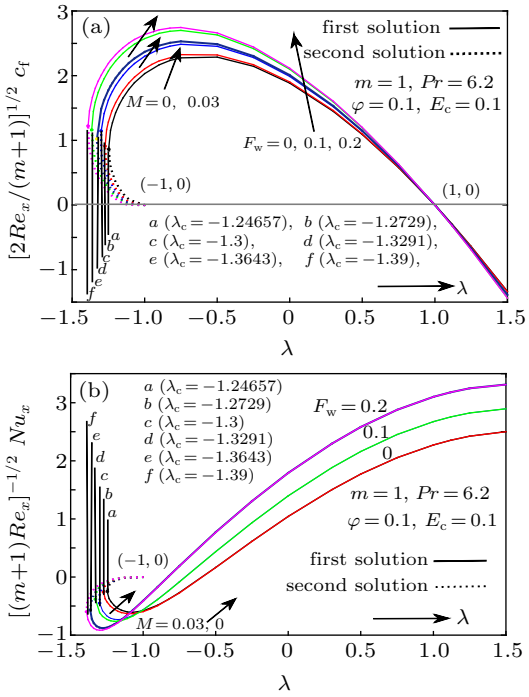


Fig. 3. (color online) Plots of shear stress (a) and temperature gradient (b) versus λ for various values of M and F_w.

Figures 4–6 show the effects of the Eckert number E_c on velocity, temperature and temperature gradient profiles for $m = 1$, $F_w = 0.1$, and $\varphi = 0.1$ in the absence ($M = 0$) and presence ($M \neq 0$) of the magnetic field inside the boundary layer. From Fig. 4, one sees that the Eckert number has a negligible effect on the velocity profiles since the parameter E_c is associated basically with the energy equation. This observation is consistent with the variation of shear stress $f''(0)$ presented in Fig. 2(a). Also, the velocity profile for magnetohydrodynamic flow is larger than that of the hydrodynamic flow for the first solution while the reverse behavior is observed for the second solution. The inset shows that the stream function $f(\eta)$ becomes negative over an increasing range of η, but for larger values of η it becomes positive and increases as η increases, i.e., the region of reverse flow appears here. From Fig. 5, one sees that an increase in magnetic field in the absence of viscous dissipation reduces the thickness of the thermal boundary layer of the Cu–water nanofluid for the first solution and the scenario is converse for the second solution. In the presence of viscous dissipation, the effect of the magnetic field is to increase the first solution of the temperature near the wall of the wedge and the reverse scenario is seen away from the wall, till it reaches the value of $\theta(\eta) = 0$ as $\eta \to \infty$. However, the opposite trend is seen for the second solution, that is, as M increases, the second solution of the temperature profiles decreases near the wall of the wedge. Moreover, the magnetic field is found to cause an overshoot in the temperature profile (i.e., the temperature profiles exceed the values at the edge of the thermal boundary layer) in the presence of viscous dissipation. However, no overshoot is observed in the temperature profiles in the absence of viscous dissipation whatever the values of the magnetic field parameter are. Also, the effect of the magnetic field is found to be more pronounced for the second solution than that for the first solution. In the absence of viscous dissipation, figure 6 shows that the temperature gradient is zero close to the surface of the wedge for some interval of η and then decreases with η rapidly till the temperature gradient reaches a negative minimum value and then increases gradually to its free surface value at η_∞ due to the reversal of heat flow between the surface and surrounding the Cu–water nanofluid, where η_∞ is relatively small for the first solution, but for the second solution, it is large. Also, it is very clear from Fig. 6 that the temperature gradient decreases near the wall of the wedge with the increase in M for the first solution but the opposite behavior is noted away from the wall, for large value of η the behavior is totally opposite for the second solution, i.e., the temperature gradient is found to increase with the increasing of M but it decreases for larger η. In the presence of viscous dissipation, the effect of the magnetic field on the temperature gradient is similar in shape to that in the absence of viscous dissipation except near the surface of the wedge where viscous dissipation dominates the heat transfer inside the thermal boundary layer. Also, the combined effect of increasing values of magnetic field and viscous dissipation is to increase initially the first solution of the temperature gradient inside the thermal boundary layer and the reverse scenario is seen away from the surface. For the second solution the behavior is opposite, i.e., the temperature gradient is found to decrease initially with the increasing of M but it increases for larger η and the thermal boundary layer thickness for the second solution is larger than that of the first solution.

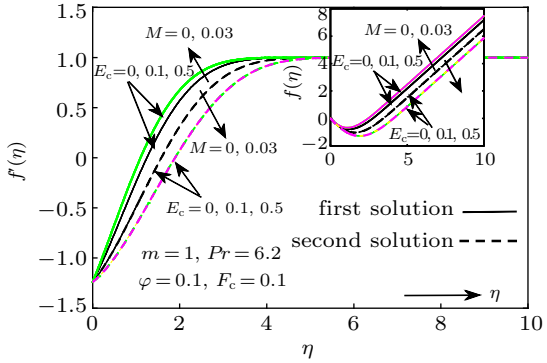


Fig. 4. (color online) Velocity profiles for various values of M and E_c.

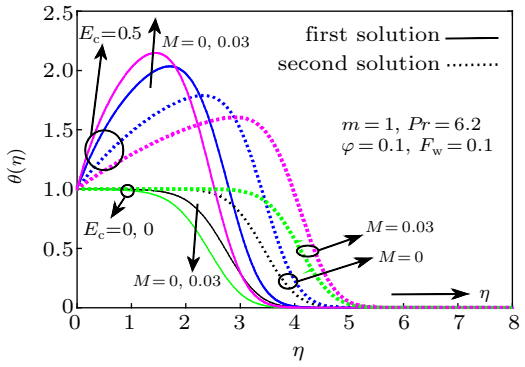


Fig. 5. (color online) Temperature profiles for various values of M and E_c.

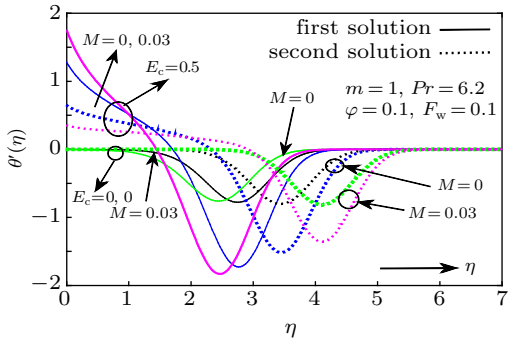


Fig. 6. (color online) Temperature gradient profiles for various values of M and E_c.

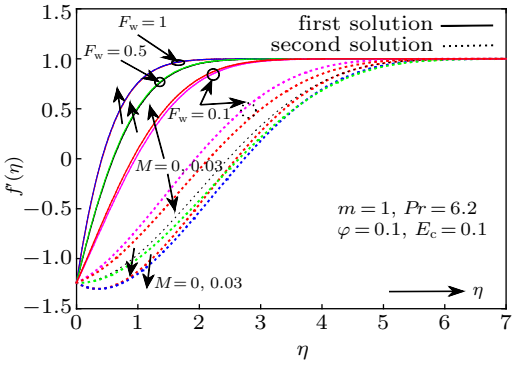


Fig. 7. (color online) Velocity profiles for various values of M and F_w.

The effects of the magnetic field and suction parameter F_w on velocity, shear stress, and temperature profiles against η for $m=1$, $\varphi=0.1$, and $E_c=0.1$ for a Cu–water nanofluid with $Pr=6.2$ are shown in Figs. 7–9. From Fig. 7, it can be seen that the velocity profile increases with the increasing of the suction parameter in the case of the first solution. This behavior is a result of the stabilizing effect of the suction on the boundary layer. It is interesting to note that the effect of the magnetic field is to increase the first solution of the velocity profile for small values of the suction parameter ($F_w \leq 0.5$) and its effect diminishes for higher values of the suction parameter ($F_w > 0.5$). However, for the second solution, the effect of the magnetic field is to reduce the velocity profile for all values of the suction parameter considered here. Further, for all values of M and F_w, the velocity becomes unity at the edge of the boundary layer, which satisfies the boundary condition and the first solution approaches unity faster than the second solution, which is compatible with the fact that the hydrodynamic boundary layer thickness for the first solution is smaller than the thickness for the second solution. This observation is in agreement with those obtained by Krishnendu.[31]

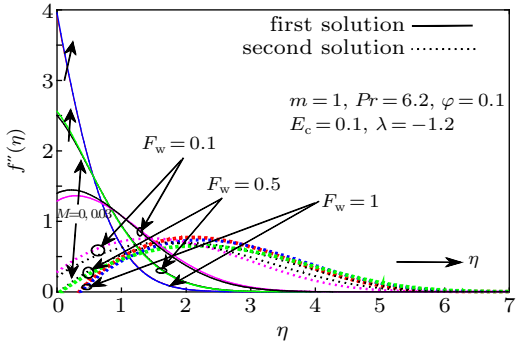


Fig. 8. (color online) Temperature gradient profiles for various values of M and F_w.

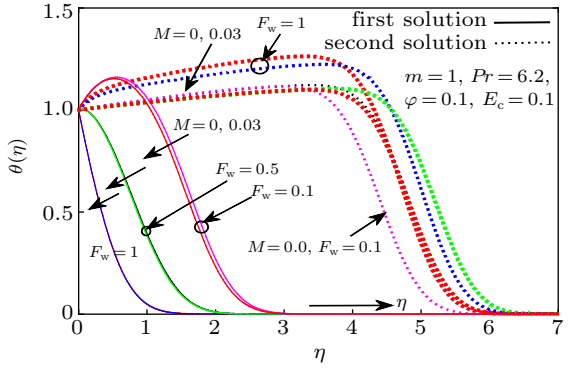


Fig. 9. (color online) Temperature profiles for various values of M and F_w.

Figure 8 shows that the shear stress may be enhanced or reduced by increasing M, depending on the fluid suction F_w. From this figure it is observed that the first solution of $f''(\eta)$ is increasing throughout the boundary layer with the increasing of M for lower values of the suction parameter ($F_w \leq 0.5$), but for larger values of the suction parameter, the magnetic field has a negligible effect on the shear stress inside the boundary layer as shown in Fig. 8. For the second solution, the shear stress initially decreases with F_w and M, but for larger η, it is not stable, therefore, it is not physically realizable. This observation is consistent with the variation of the velocity profile in Fig. 7. From Fig. 9, it can be seen that suction reduces the temperature profiles in the first solution because the increments of the thermal boundary and the temperature of the Cu–water nanofluid near the wall exceed those at the wall for the small values of the suction parameter, i.e., temperature overshoot occurs throughout the thermal boundary layer. On the other hand, it may be seen that when the magnetic field parameter increases, the first solution of the temperature profile decreases for small values of the suction parameter ($F_w \leq 0.5$)

and its effect diminishes for higher values of the suction parameter ($F_w > 0.5$) while the second solution is not stable and, therefore, it is not physically realizable.

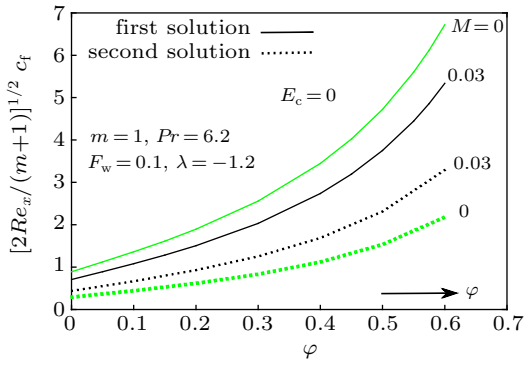


Fig. 10. (color online) Plots of shear stress versus φ for various values of M with $E_c = 0$.

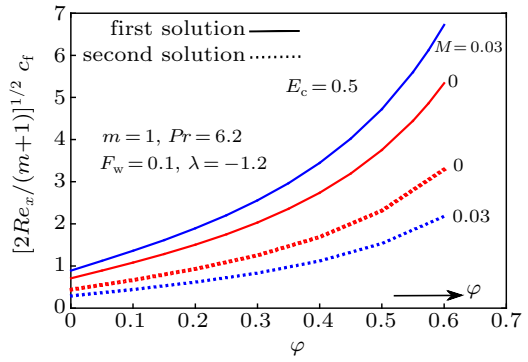


Fig. 11. (color online) Plots of shear stress versus φ for various values of M with $E_c = 0.5$.

Figures 10 and 11 illustrate the local friction coefficients each as a function of the volume friction parameter φ for $E_c = 0$ (in the absence of viscous dissipation) and 0.5 (in the presence of viscous dissipation), respectively, with $M = 0$ (hydrodynamic nanofluid) and 0.03 (magnetohydrodynamic nanofluid). We notice that as the volume friction parameter increases, the friction coefficient also increases in the absence as well as in the presence of the viscous dissipation parameter E_c. We also notice that for $E_c = 0$, the first solution of the friction coefficient decreases with M, but the opposite case happens for the second solution. However, when $E_c \neq 0$, we notice that the trend is to be *vice versa*, that is as M increases, the friction coefficient increases for the first solution, but for the second solution, the friction coefficient decreases as M increases. Figure 12 shows that the maximum differences in Nusselt number distribution among various values of M occur under larger values of the volume friction parameter φ, and these differences are almost negligible for $\varphi = 0$ (regular fluid). This is because the presence of nanoparticles in the fluid without viscous dissipation increases appreciably the effective thermal conductivity of the fluid and consequently enhances the heat transfer characteristics. However, in the presence of viscous dissipation ($E_c \neq 0$), figure 13 shows that the Nusselt number becomes negative for all values of φ, indicating the reversal of the direction of heat transfer from the initial wall to fluid (which can also be understood by the corresponding overshoot in the temperature profiles due to presence of viscous dissipation).

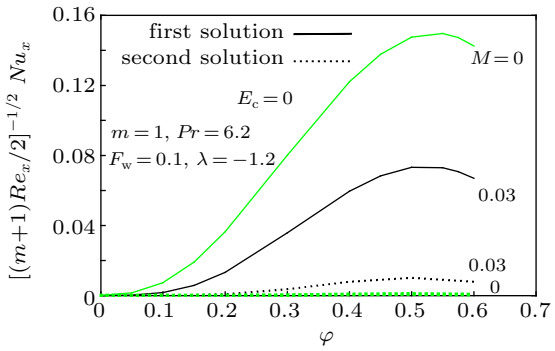


Fig. 12. (color online) Plots of temperature gradient versus φ for various values of M with $E_c = 0$.

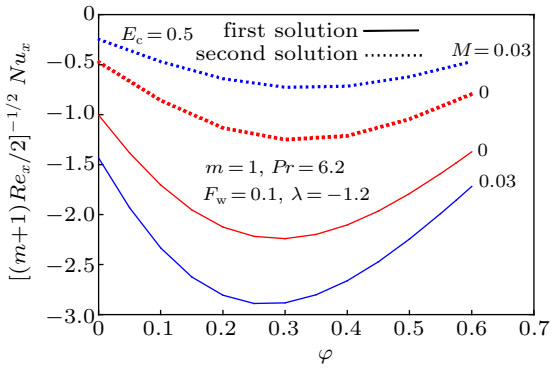


Fig. 13. (color online) Plots of temperature gradient versus φ for various values of M with $E_c = 0.5$.

4. Conclusions

The problem of boundary layer flow of a copper (Cu)–water-based nanofluid over a moving wedge is investigated numerically. The governing partial differential equations are first transformed into a system of ordinary differential equations using a similarity transformation and then solved numerically by using Runge–Kutta and shooting method. The effects of the solid volume fraction φ, velocity ratio parameter λ, magnetic field parameter M, suction parameter F_w, and the viscous dissipation parameter E_c on flow and heat transfer characteristics are determined for the Cu–water nanofluid. The numerical results obtained accord very well with the previous data for some particular cases of the present study. Dual similarity solutions for the velocity field and also for the temperature distribution are obtained for some negative values of the velocity ratio parameter λ (the wedge and the free stream velocity move in the opposite directions). The solution does not exist beyond a certain critical value of λ. This critical value of λ depends on the values of the suction parameter and the magnetic field. It is observed that the suction and magnetic field increase the range

of λ ($\lambda < 0$) for which the dual solution exists. At the positions very close to the surface of the wedge, the stream function $f(\eta)$ takes negative values which means that in that region, the flow is reversed. Also, the obtained numerical results show that the first solution of the dimensional stream function of the Cu–water nanofluid is greater in the magnetohydrodynamic case than in the hydrodynamic one. Analyses of the results show that the effect of magnetic field is to increase the first solution of the velocity profile and reduce the first solution of the temperature profile. But this effect becomes negligible when the suction parameter is large. On the other hand, the effect of viscous dissipation is to increase the first solution of the temperature profile inside the thermal boundary layer. However, maximum enhancement of temperature due to the application of the magnetic field occurs when the wall of the wedge is porous and subjected to the suction of the fluid.

References

[1] Choi S U S 1995 *ASME International Mechanica Engineering Congress and Exposition*, San Francsco, USA, ASME, FED 231/MD 99

[2] Wong K F V and Leone O D 2010 *Applications of Nanofluids: Current and Future, Adv. Mech. Eng.* 2010: 519659

[3] Khanafer K, Vafai K and Lightstone M 2003 *J. Heat Mass Transfer* **46** 3639

[4] Maiga S E B, Palm S J, Nguyen C T, Roy G and Galanis N 2005 *Int. J. Heat Fluid Flow* **26** 530

[5] Jou R Y and Tzeng S C 2006 *Int. Commun. Heat Transfer* **33** 727

[6] Tiwari I K and Das M K 2007 *Int. J. Heat Mass Transfer* **50** 2002

[7] Hang K S, Lee Ji H and Jang S P 2007 *Int. J. Heat Mass Transfer* **50** 4003

[8] Oztop H F and Abu-Nada E 2008 *Int. J. Heat Fluid Flow* **29** 1326

[9] Muthtamilselvan M, Kandaswamy P and Lee J 2010 *Commun. Nonlinear Sci. Numer. Simul.* **15** 1501

[10] Buongiorno J 2006 *ASME J. Heat Transfer* **128** 240

[11] Kuznetsov A V and Nield D A 2010 *Int. J. Therm. Sci.* **49** 243

[12] Abu-Nada E and Oztop H F 2009 *Int. J. Heat Fluid Flow* **30** 669

[13] Riley N and Weidman P D 1989 *SIAM J. Appl. Math.* **49** 1350

[14] Yacob N A, Ishak A I and Pop I 2011 *Int. J. Thermal Sci.* **50** 133

[15] Falkner V M and Skan S W 1931 *Phil. Mag.* **12** 865

[16] Devi A and Kandasamy R 2002 *Int. Commun. Heat Mass Transfer* **29** 707

[17] Kandasamy R M, Azme B and Rozaini R 2012 *Int. J. Thermal Sci.* **65** 196

Kandasamy R and Anjali Dev S P 2002 *J. Energy, Heat Mass Transfer* **24** 175

[18] Kumari M 1998 *Int. J. Engin. Sci.* **36** 299

[19] Bachok N, Ishak A and Pop I 2010 *Int. J. Thermal Sci.* **49** 1663

[20] Xiaohong S W, Zheng L, Zhang X and Zhang J 2012 *Chem. Engin. Sci.* **78** 1

[21] Hamad M A A, Pop I and Ismail A I 2011 *Nonlinear Analysis: Real World Applications* **12** 1338

[22] Gebhart B 1962 *J. Fluid Mech.* **14** 225

[23] Pantokratoras A 2004 *Appl. Math. Model.* **6** 553

[24] Zueco J and Beg O A 2009 *Math. Comput. Model.* **50** 439

[25] Muhaimin I, Kandasamy R, Hashim I and Ruhaila 2008 *Int. J. Appl. Math. Statistics* **13** 9

[26] Chandrasekar M and Baskaran S 2007 *Theor. Appl. Mech.* **34** 197

[27] Makinde O D 2012 *Appl. Math. Mech.* **33** 1442

[28] Na T Y 1974 *Computational Method in Engineering Boundary Value Problems* (New York: Academic Press)

[29] Wang C Y 2008 *Int. J. Nonlinear Mech.* **43** 377

[30] Bachok N, Ishak A and Pop I 2010 *Phys. Lett. A* **347** 4075

[31] Krishnendu B 2011 *Int. Commun. Heat Mass Transfer* **38** 917